

HiggsTools: BSM scalar phenomenology with new versions of HiggsBounds and HiggsSignals

Henning Bahl¹, Thomas Biekötter², Sven Heinemeyer³, Cheng Li⁴, Steven Paasch⁴,
 Georg Weiglein^{4,5}, and Jonas Wittbrodt⁶

¹ *University of Chicago, Department of Physics and Enrico Fermi Institute,
 5720 South Ellis Avenue, Chicago, IL 60637 USA*

² *Institute for Theoretical Physics, Karlsruhe Institute of Technology, Wolfgang-Gaede-Str. 1,
 76131 Karlsruhe, Germany*

³ *Instituto de Física Teórica, (UAM/CSIC), Universidad Autónoma de Madrid,
 Cantoblanco, E-28049 Madrid, Spain*

⁴ *Deutsches Elektronen-Synchrotron DESY, Notkestr. 85, 22607 Hamburg, Germany*

⁵ *II. Institut für Theoretische Physik, Universität Hamburg, Luruper Chaussee 149, 22761
 Hamburg, Germany*

⁶ *Department of Astronomy and Theoretical Physics, Lund University, Sölvegatan 14A, 223 62
 Lund, Sweden**

Abstract

The codes **HiggsBounds** and **HiggsSignals** compare model predictions of BSM models with extended scalar sectors to searches for additional scalars and to measurements of the detected Higgs boson at 125 GeV. We present a unification and extension of the functionalities provided by both codes into the new **HiggsTools** framework. The codes have been re-written in modern C++ with native Python and Mathematica interfaces for easy interactive use. We discuss the user interface for providing model predictions, now part of the new sub-library **HiggsPredictions**, which also provides access to many cross sections and branching ratios for reference models such as the SM. **HiggsBounds** now implements experimental limits purely through json data files, can better handle clusters of BSM particles of similar masses (even for complicated search topologies), and features an improved handling of mass uncertainties. Moreover, it now contains an extended list of Higgs-boson pair production searches and doubly-charged Higgs boson searches. In **HiggsSignals**, the treatment of different types of measurements has been unified, both in the χ^2 computation and in the data file format used to implement experimental results.

emails: hbahl@uchicago.edu, thomas.biekoetter@desy.de, Sven.Heinemeyer@cern.ch, cheng.li@desy.de,
 steven.paasch@desy.de, georg.weiglein@desy.de, jonas.wittbrodt@desy.de

*Former address.

Contents

1	Introduction	2
2	The HiggsTools framework	3
2.1	HiggsPredictions	3
2.1.1	Process definitions	3
2.1.2	Tabulated cross sections and branching ratios	5
2.2	HiggsBounds	8
2.2.1	Limit types	8
2.2.2	Particle clustering	9
2.2.3	Treatment of mass uncertainties	10
2.2.4	Higgs pair production limits	11
2.2.5	Doubly-charged Higgs bosons	12
2.3	HiggsSignals	12
3	C++, Python, and Mathematica interfaces	13
3.1	Installation	13
3.2	The C++ and Python interfaces	14
3.2.1	User input via HiggsPredictions	14
3.2.2	Running HiggsBounds	16
3.2.3	Running HiggsSignals	17
3.3	Mathematica	18
4	Examples	19
4.1	Constraining the charm Yukawa coupling with HiggsSignals	19
4.2	Sensitivity comparison of resonant h_{125} -pair production with HiggsBounds	21
4.3	Constraining the width of the h_{125} Higgs boson with HiggsSignals	23
4.4	Constraining the 2HDM	25
5	Conclusions	28

1 Introduction

With the discovery of a Higgs boson with a mass of ~ 125 GeV at the LHC [1, 2], the first (potentially) elementary scalar particle was observed. This discovery marks an important milestone in the quest to unravel the nature of electroweak symmetry breaking (EWSB). The further investigation of EWSB — i.e., the precise determination of the properties of the Higgs boson at 125 GeV as well as the search for additional scalar bosons — is one of the main tasks of the LHC physics program.

Many models beyond the SM (BSM) contain extensions of the Standard Model (SM) Higgs-boson sector, thus predicting additional scalar particles. Well-known examples include the extension of the SM Higgs sector by additional $SU(2)_L$ singlets, doublets and also higher representations. The LHC searches carried out so far have not led to the discovery of additional scalar bosons. Correspondingly, the searches have resulted in exclusion limits constraining the parameter space of BSM models with extended scalar sectors.

Similarly, measurements of the properties of the Higgs boson at 125 GeV so far have not found any conclusive deviation from the SM predictions. In turn, also these measurements constrain the parameter space of BSM models which naturally predict modifications of the couplings of the Higgs boson at 125 GeV (commonly called the “SM-like Higgs boson”) w.r.t. the corresponding SM predictions.

Consequently, every BSM model modifying the scalar sector of the SM — either by modifying the couplings of the SM-like Higgs boson or by adding new BSM scalars to the theory — should be tested against all the available data collected at the LHC, at LEP and other colliders. Due to the large number of available searches and measurements, checking the consistency of a BSM parameter point with these experimental results is not feasible without the development of dedicated computer tools to facilitate this task.

The codes `HiggsBounds` [3–6] (see also Ref. [7]) and `HiggsSignals` [8, 9] have been developed in this spirit. While `HiggsBounds` allows checking BSM models against exclusion limits from searches for new scalar bosons, `HiggsSignals` allows one to check the compatibility of the model with the LHC rate measurements of the Higgs boson at 125 GeV. Both codes, which were written using `Fortran`, have been developed and extended for roughly one decade.

In this paper, we present a complete rewrite of `HiggsBounds` and `HiggsSignals` in modern `C++`. `HiggsBounds` and `HiggsSignals` are now parts of the package `HiggsTools` which also contains `HiggsPredictions` as a third subpackage facilitating for the user the task of providing theory predictions for the production and decay rates of BSM scalar bosons from the model input. The new setup allows for an easy implementation of new searches and measurements and provides simple-to-use `C++`, `Python`, and `Mathematica` interfaces. It also contains new features like the implementation of non-resonant di-Higgs boson searches, the support for doubly-charged Higgs bosons, or \mathcal{CP} -sensitive coupling measurements. In this paper we provide a description of the updated codes as well as the newly implemented search limits and rate measurements, and we illustrate the application to several physics examples, demonstrating these new features.

The paper is structured as follows. In Section 2, we discuss the `HiggsTools` framework containing the three subpackages `HiggsPredictions`, `HiggsBounds`, and `HiggsSignals`. Instructions on how to use this framework are given in Section 3. In Section 4, we present

several physics examples demonstrating the features of the `HiggsTools` framework. Our conclusions are provided in Section 5.

2 The HiggsTools framework

The `HiggsTools` framework represents a unification and extension of the codes `HiggsBounds` and `HiggsSignals`. Moreover, it includes the new sub-library `HiggsPredictions` handling the user input and providing access to many relevant cross sections and branching ratios.

Correspondingly, the `HiggsTools` package contains three subpackages,

- `HiggsPredictions` for defining the physical model and obtaining theory prediction for production and decay rates,
- `HiggsBounds` for evaluating bounds from direct searches for scalar particles,
- `HiggsSignals` for evaluating compatibility with the measurements of the Higgs boson detected at ~ 125 GeV.

In the following, we will describe the different subpackages in more detail with a special focus on new features with respect to older version of `HiggsBounds` and `HiggsSignals`.

2.1 HiggsPredictions

`HiggsPredictions` allows defining the physical model. This means that the user has to specify the scalar content of the model and the properties of each BSM scalar.

These properties include

- the mass and total width (including theoretical mass uncertainties),
- the electric charge and \mathcal{CP} character,
- the rates of all relevant production and decay modes (at LEP and the LHC).

All these properties can be set by the user explicitly. Alternatively, the effective coupling input [6] can be used to automatically obtain predictions for the most relevant production and decay modes. Moreover, SLHA files or `HiggsBounds` data files [6] can be used as input via the `Python` interface.

2.1.1 Process definitions

All relevant direct searches for BSM scalars as well as the measurements of the properties of the Higgs boson at 125 GeV are implemented based on the concept of processes.

`HiggsTools` currently supports four different types of processes (as depicted in Fig. 1):

- channel processes,
- chain decay processes,
- pair decay processes,

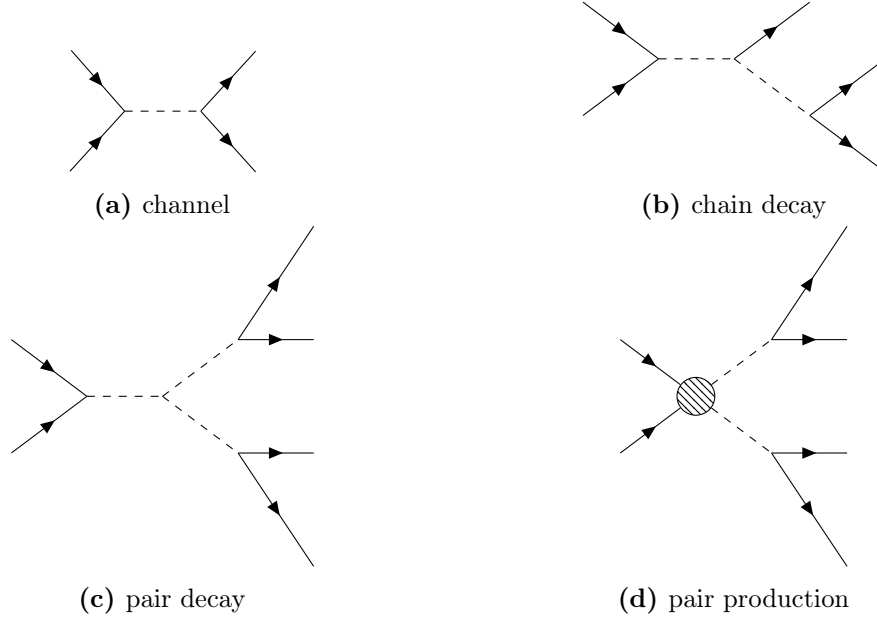


Figure 1: Overview of the different process types used within in **HiggsTools**.

- pair production processes.

The channel process is the simplest type of process. It is used for collider processes for which a single (BSM) scalar is produced with specific initial and final states consisting of SM particles. An example process is Higgs production via gluon fusion and the subsequent decay to two photons, $gg \rightarrow H \rightarrow \gamma\gamma$.

The second type of process is the chain decay process. This process type involves two BSM scalars. The first BSM scalar is produced and then decays to the second BSM scalar and SM particles. The second BSM scalar subsequently decays to SM particles. A typical example is the production of a \mathcal{CP} -odd Higgs boson via gluon fusion followed by a decay to a \mathcal{CP} -even Higgs boson and a Z boson with the second Higgs bosons decaying to bottom quarks, $gg \rightarrow A \rightarrow ZH \rightarrow Zb\bar{b}$.

The pair decay process extends the chain decay process by a third BSM scalar. The first scalar is produced via a SM initial state and decays into two BSM scalars which subsequently decay to SM particles. One example would be the decay of the SM-like Higgs boson into two light \mathcal{CP} -odd Higgs bosons, which then decay to bottom quarks and two photons, $pp \rightarrow h_{125} \rightarrow aa \rightarrow b\bar{b}\gamma\gamma$.

Two BSM scalars can, however, also be produced without originating from the decay of an initial scalar. This possibility is covered by the pair production process which is used for the production of two BSM scalars from a SM initial state and the subsequent decays into SM particles. Typical examples are searches for pair-produced Higgs bosons (performed without the assumption of an initial resonance), e.g. $pp \rightarrow h_1 h_2 \rightarrow b\bar{b}\gamma\gamma$.

The user does not need to provide predictions for every single process. Instead, it is sufficient to input the production cross sections and branching ratios of the relevant scalars. **HiggsPredictions** will then automatically obtain predictions for every process for which a limit is implemented.

In this procedure, **HiggsPredictions** will automatically take into account necessary symmetry factors. This is especially relevant for the pair decay and pair production processes, for which two BSM particles h_i and h_j appear in the final state. Assuming that h_i and h_j decay into the sets of final states $A = \{a_1, a_2, \dots\}$ and $B = \{b_1, b_2, \dots\}$, respectively, their combined decay rate is given by

$$\text{Br}(h_i h_j \rightarrow AB) = \begin{cases} \sum_{a \in A} \sum_{b \in B} \text{Br}(h_i \rightarrow a) \text{Br}(h_j \rightarrow b) & i \neq j, \\ \sum_{\{a,b\} \forall a \in A, b \in B} S(\{a,b\}) \text{Br}(h_i \rightarrow a) \text{Br}(h_i \rightarrow b) & i = j. \end{cases} \quad (1)$$

The sum in the second case runs over all unique unordered pairs $\{a,b\}$, and the symmetry factor S is

$$S(\{a,b\}) = \begin{cases} 1 & a = b, \\ 2 & a \neq b. \end{cases} \quad (2)$$

For example, if $A = \{bb, \tau\tau\}$ and $B = \{bb, \gamma\gamma\}$ the result would be

$$\text{Br}(h_i h_j \rightarrow AB) = \begin{cases} \text{Br}_{bb}^i \text{Br}_{bb}^j + \text{Br}_{bb}^i \text{Br}_{\gamma\gamma}^j + \text{Br}_{\tau\tau}^i \text{Br}_{bb}^j + \text{Br}_{\tau\tau}^i \text{Br}_{\gamma\gamma}^j & i \neq j \\ (\text{Br}_{bb}^i)^2 + 2 \text{Br}_{bb}^i \text{Br}_{\gamma\gamma}^i + 2 \text{Br}_{\tau\tau}^i \text{Br}_{bb}^i + 2 \text{Br}_{\tau\tau}^i \text{Br}_{\gamma\gamma}^i & i = j, \end{cases} \quad (3)$$

where $\text{Br}_a^i = \text{Br}(h_i \rightarrow a)$. Permutations of h_i and h_j when $i \neq j$ are not included at this stage, but are instead accounted for by sums over the corresponding particle clusters C_1, C_2 ,

$$\text{Br}(C_1 C_2 \rightarrow AB) = \sum_{h_i \in C_1} \sum_{h_j \in C_2} \text{Br}(h_i h_j \rightarrow AB). \quad (4)$$

See Section 2.2.2 for a detailed discussion of the meaning of particle clusters.

It should be noted that in this branching ratio calculation, electrically charged particle–antiparticle pairs have to be treated as distinct. For this reason, **HiggsPredictions** currently only allows the implementation of overall neutral final states for pair decay or pair production processes (including final states with two opposite charged BSM scalars).

2.1.2 Tabulated cross sections and branching ratios

While production cross section and branching ratio values can completely be provided by the user, **HiggsPredictions** also provides tabulated reference model predictions for the most common Higgs production and decay channels.

The largest set of predictions is available for scalar bosons with exactly the same couplings as the SM Higgs boson. The tabulated cross section and branching ratio values then only depend on the mass of the new scalar. The numbers for this SM reference model are taken from Ref. [10]. For the production cross sections, the following channels are available:

- $gg \rightarrow H$,
- $pp \rightarrow b\bar{b}H$,
- $pp \rightarrow H + 2j$ (VBF),

- $pp \rightarrow WH$,
- $pp \rightarrow ZH$ (including $gg \rightarrow ZH$, $qq \rightarrow ZH$, $b\bar{b} \rightarrow ZH$),
- $pp \rightarrow t\bar{t}H$,
- $pp \rightarrow tH$ (t channel + s channel),
- tWH .

All these cross sections are available for scalar masses ranging from 10 GeV to 3 TeV and take state-of-art QCD corrections into account. For the masses between 120 GeV and 130 GeV also predictions including electroweak corrections are available.

Similarly, branching ratio predictions are available for the following decay modes:

- $H \rightarrow c\bar{c}, s\bar{s}, t\bar{t}, b\bar{b}$,
- $H \rightarrow \tau^+\tau^-, \mu^+\mu^-$,
- $H \rightarrow W^{(*)}W^{(*)}, Z^{(*)}Z^{(*)}, Z\gamma, \gamma\gamma, gg$,
- $H \rightarrow \text{invisible}$.

In Ref. [10], numbers are given for masses between 20 GeV and 900 GeV. We extended this mass range to the interval 1 – 1000 GeV using `HDecay` [11, 12]. In addition, we added predictions for the $H \rightarrow s\bar{s}$ decay channel also using `HDecay`. Predictions including electroweak corrections are available in the mass range [120, 130] GeV.

In addition to these predictions for scalars with SM-like couplings, `HiggsPredictions` also implements predictions for scalars with a non-SM-like coupling structure (or non-SM-like quantum numbers). These are available for the most relevant production modes and encode the dependence on the most relevant couplings. On the other hand, effects from other BSM particles appearing in the production process at the tree or loop level are not taken into account. These cross section predictions can either be directly accessed or automatically used by employing the effective coupling input.

An overview of the implemented cross section predictions for scalars with a non-SM-like coupling structure is given in Table 1. The code `SusHi` 1.7.0 [16, 17] has been used to derive the cross section for Higgs production via gluon fusion; for the VBF channel, the code `HAWK` 3.0.0 [18–21] has been employed; the top-associated Higgs production cross sections have been derived employing the code `MadGraph5_aMC@NLO` 2.8.2 [22] using the `MSTW2008LO` [23] PDF set assessed via the `LHAPDF` 6.2.3 interface [24]; and for the vector-boson associated Higgs production cross sections, we employed the code `vhnnlo` 2.1 [25, 26] (cross-checked with `MadGraph` [27]).

If not stated otherwise, all cross section predictions are available only for the 13 TeV LHC. In Table 1, c_Z and c_W denote the couplings of the scalar to Z and W bosons normalized to the respective coupling of the SM Higgs boson (see Ref. [6] for more details). Similarly, c_q and \tilde{c}_q denote the \mathcal{CP} -even and \mathcal{CP} -odd Yukawa couplings to the quark q , which are both normalized to the respective \mathcal{CP} -even SM Yukawa coupling (see Ref. [6] for more details). $c_{q,ij}$ and $\tilde{c}_{q,ij}$ are used to denote potentially flavor-violating Yukawa couplings to the quarks

prod. channel	coupling dep.	mass range [GeV]	source
ggH	$c_t, \tilde{c}_t, c_b, \tilde{c}_b$	10 – 3000	SusHi
bbH	c_b, \tilde{c}_b	10 – 3000	resc. of SM result
VBF	c_Z, c_W	LHC8: 1 – 1050, LHC13: 1 – 3050	HAWK
$t\bar{t}H$	c_t, \tilde{c}_t	25 – 1000	MadGraph
tH (t channel)	c_t, \tilde{c}_t, c_W	25 – 1000	MadGraph
tWH	c_t, \tilde{c}_t, c_W	25 – 1000	MadGraph
WH	c_W, c_t	1 – 2950	vh@nnlo
$qq \rightarrow ZH$	c_Z, c_t	1 – 5000	vh@nnlo
$gg \rightarrow ZH$	$c_t, c_b, c_Z, \tilde{c}_t, \tilde{c}_b$	1 – 5000	vh@nnlo
$b\bar{b} \rightarrow ZH$	c_b	1 – 5000	vh@nnlo
$q_i q_j \rightarrow H$	$c_{q,ij}, \tilde{c}_{q,ij}$	1 – 5000	vh@nnlo
$q_i q_j \rightarrow H^\pm$	$c_{qL,ij}, c_{qR,ij}$	200 – 1150	Ref. [7]
$q_i q_j \rightarrow H + \gamma$	$c_{q,ij}, \tilde{c}_{q,ij}$	200 – 1150	Ref. [7]
$q_i q_j \rightarrow H^\pm + \gamma$	$c_{qL,ij}, c_{qR,ij}$	200 – 1150	Ref. [7]
$b\bar{b} \rightarrow ZH$	c_b	200 – 1150	Ref. [7]
$pp \rightarrow H^\pm tb$	$c_{L,tb}, c_{R,tb}$	145 – 2000	Refs. [13, 14]
$pp \rightarrow H^\pm \phi$	$c_{H^\pm \phi W^\mp}$	$m_\phi : 10 - 500, m_{H^\pm} : 100 - 500$	Ref. [15]

Table 1: Overview of cross section predictions available in `HiggsPredictions` for scalars with a non-SM-like coupling structure.

q_i and q_j , for which only the diagonal couplings are normalized to the respective SM values (see Ref. [7] for more details). For charged scalars, $c_{qL,ij}$ and $c_{qR,ij}$ are used to denote the left- and right-handed couplings of the charged scalars to the quarks q_i and q_j (see Ref. [7] for more details). $c_{H^\pm \phi W^\mp}$ denotes the coupling of a charged scalar to a neutral scalar ϕ and a W boson (see Ref. [15]).

All cross sections are calculated automatically by `HiggsPredictions` if the corresponding effective couplings are used as input. In order to incorporate higher-order corrections in an approximate way, we normalize the fitted cross sections σ_{fit} by the corresponding cross section evaluated for a Higgs boson with SM-like couplings. The derived number is then multiplied with the respective SM prediction $\sigma_{\text{SM}}^{\text{YR4}}$ from Ref. [10]. This procedure can be summarized in the equation

$$\sigma(m, c_i) = \frac{\sigma_{\text{fit}}(m, c_i)}{\sigma_{\text{fit}}(m, c_i^{\text{SM}})} \sigma_{\text{SM}}^{\text{YR4}}(m), \quad (5)$$

where c_i denotes the set of effective couplings and c_i^{SM} the corresponding prediction for a SM Higgs boson.

With respect to the previous implementation of the effective coupling input in `HiggsBounds-5`, we have improved the handling of heavy Higgs decays to two top quarks. Previously, the decay rates of a \mathcal{CP} -even SM-like Higgs boson given in Ref. [10] were rescaled by the absolute value of the effective top-Yukawa coupling, $c_t^2 + \tilde{c}_t^2$. This rescaling factor is valid in the limit where the ratio $m_H^2/(4m_t^2)$ is negligible, where m_H is the mass of the decaying Higgs boson and m_t is the top-quark mass. Going beyond this approximation, the

decay rate of a heavy Higgs boson to two top quarks is proportional to

$$\Gamma_{H \rightarrow t\bar{t}} \propto c_t^2 \beta_t^3 + c_{\bar{t}}^2 \beta_t \quad \text{with} \quad \beta_t = \sqrt{1 - \frac{m_H^2}{4m_t^2}}. \quad (6)$$

Those different scalings of the parts proportional to the \mathcal{CP} -even and \mathcal{CP} -odd top-Yukawa couplings are now taken into account in **HiggsPredictions**. In comparison to **HiggsBounds-5**, this results in increased branching ratios to top quarks for \mathcal{CP} -odd Higgs boson with a mass close to the $t\bar{t}$ threshold.

2.2 HiggsBounds

HiggsBounds checks the process rates computed by **HiggsPredictions** based on the input on the considered model provided by the user against a database of experimental limits. For every of these limits, **HiggsBounds** performs the following steps:

- check which particles in the model are relevant for each role in the process,
- find all maximal clusters for each role that fulfil the analysis assumptions,
- for all assignments of clusters to the process roles compute the channel rate based on the model predictions provided by **HiggsPredictions**,
- obtain the observed and expected ratios.

Then, the most sensitive limit for each particle is selected based on the highest expected ratio. The parameter point is then regarded as allowed if the observed ratio is smaller than one for the most sensitive limit for each particle. This procedure, which has been adopted in order to allow a well-defined statistical interpretation of the applied limit, is described in more detail in Refs. [3–6].

At the moment, the **HiggsBounds** limit database contains 258 different experimental limits from LEP and the LHC.

2.2.1 Limit types

The main new feature of the new **HiggsBounds** implementation, **HiggsBounds-6**, is a much easier way to incorporate new experimental limits. The whole information about every limit is now encoded in a **json** file.¹ In the initialization step of **HiggsBounds**, a user-specified set of these **json** files is read-in and then used for the limit setting.² For the limit implementation (and evaluation), six different limit types are differentiated:

- Channel limit

A 95% C.L. limit on the rate of a channel process that only depends on the mass of the particle.

Example: ATLAS search for a heavy Higgs boson produced in association with bottom quarks and decaying into bottom quarks ($pp \rightarrow b\bar{b}h_{\text{BSM}} \rightarrow b\bar{b}b\bar{b}$) [29].

¹This includes non-trivial acceptance functions as for example used in Ref. [7].

²For a detailed description of the file format, we refer to Ref. [28]

- Channel width limit

A 95% C.L. limit on the rate of a channel process that only depends on the mass and width of the particle.

Example: CMS search for a scalar resonance decaying to a pair of Z bosons ($pp \rightarrow h_{\text{BSM}} \rightarrow ZZ$) [30].

- Chain decay limit

A 95% C.L. limit on the rate of a chain decay process that only depends on the masses of the involved BSM particles.

Example: CMS search for a heavy Higgs boson decaying to a Z boson and a SM-like Higgs boson ($gg \rightarrow h_{\text{BSM}} \rightarrow h_{125}Z \rightarrow b\bar{b}\ell^+\ell^-$) [31].

- Pair decay limit

A 95% C.L. limit on the rate of a pair decay process that only depends on the masses of the involved BSM particles.

Example: CMS search for a heavy Higgs boson decaying to two SM-like Higgs bosons ($pp \rightarrow h_{\text{BSM}} \rightarrow h_{125}h_{125} \rightarrow b\bar{b}\tau^+\tau^-$) [32].

- Pair production limit

A 95% C.L. limit on the rate of a pair production process that only depends on the masses of the involved BSM particles.

Example: LEP search for pair production of two Higgs bosons ($e^+e^- \rightarrow h_1h_2 \rightarrow b\bar{b}\tau^+\tau^-$) [33].

- Likelihood limit

A limit expressed as a likelihood profile on the rate of multiple channel processes and the mass of the particle.

Example: CMS search for heavy Higgs bosons decaying into two tau leptons which are either produced via gluon fusion or in association with bottom quarks [34].

After reading-in the limit database, **HiggsBounds** assigns the BSM scalars and their process rates as provided by **HiggsPredictions** to specific limits.

2.2.2 Particle clustering

For each specific limit, all scalars which could participate in the corresponding process are identified. As an example, for the channel process $pp \rightarrow \phi \rightarrow b\bar{b}$ the role of ϕ within the considered model could be played by h_1 or h_2 . Then, the set $\{h_1, h_2\}$ is called a particle cluster.

We define a cluster C of particles with masses m_1, \dots, m_i to be valid if

$$\max(m_1, \dots, m_i) - \min(m_1, \dots, m_i) \leq r_{\text{abs}} + r_{\text{rel}} \cdot \text{mean}(m_1, \dots, m_i), \quad (7)$$

where r_{abs} and r_{rel} are the absolute and relative experimental resolutions, respectively. These are either given by the experiment or estimated. In the simple case of a channel limit on

$pp \rightarrow \phi \rightarrow b\bar{b}$, the limit is then evaluated at the rate-weighted mass and the rate-weighted total width of all particles in the cluster.

This clustering algorithm has been used already in previous versions of `HiggsBounds/HiggsSignals`, and more details can be found in Refs. [6, 35]. The new implementation in `HiggsTools` extends this functionality by forming clusters for processes involving more than one type of BSM scalars (e.g. $pp \rightarrow \phi_i \rightarrow h_{125}\phi_j, h_{125} \rightarrow \tau^+\tau^-, \phi_j \rightarrow b\bar{b}$). In this case, clusters for every BSM particle are formed following the steps outlined above. The limit is then evaluated at the rate-weighted masses and total widths of the clusters formed for ϕ_i and ϕ_j .

As an example, we consider a BSM model containing the \mathcal{CP} -even scalars h, H, S and the \mathcal{CP} -odd scalars A, A_S (as e.g. in the N2HDM) with the mass hierarchy $m_H \sim m_A > m_h \sim m_S \sim m_{A_S}$. Then, possible decay modes — assuming \mathcal{CP} conservation — are $H \rightarrow hh, SS, hS, A_S A_S$ and $A \rightarrow hA_S, SA_S$. The clustering algorithm would then potentially assign H and A to one cluster used to compute the mass and width of ϕ_i as well as S and A_S to one cluster used to compute the mass and width of ϕ_j .

2.2.3 Treatment of mass uncertainties

A further improvement of `HiggsBounds` with respect to previous versions is the handling of mass uncertainties. In many BSM theories, not all scalar masses are input quantities. Instead, the masses can be calculated in terms of the model parameters (see e.g. Ref. [36] for a discussion of Higgs mass predictions in the Minimal Supersymmetric extension of the SM). These theoretical predictions are affected by theoretical and parametric uncertainties induced by unknown higher-order corrections and an imprecise knowledge of the input quantities, respectively.

In previous versions of `HiggsBounds`, mass uncertainties have been handled by running the `HiggsBounds` algorithm multiple times. For a single scalar with mass uncertainty, the `HiggsBounds` algorithm was executed three times: once for the central mass value, once for the central mass value minus the mass uncertainty, and once for the central mass value plus the mass uncertainty. In the end, the result of the run with the weakest constraints was returned. In the case of multiple scalars with mass uncertainties, the `HiggsBounds` algorithm was executed for all possible combinations of the central masses plus/minus the associated uncertainties resulting in 3^n runs with n being the number of scalars with a mass uncertainty.

The new version of `HiggsBounds` improves the handling of mass uncertainties in the following way. As explained, `HiggsBounds` only applies the limit with the largest expected ratio. In order to determine the mass value at which each limit is evaluated, the mass is varied within the user-given uncertainty range (checking also intermediate values). Then, the mass with the lowest observed ratio is selected. At this point, also the expected ratio used to compare the sensitivity between the different limits is evaluated.

The usefulness of this prescription becomes clear when discussing experimental searches before the Higgs discovery. Many of these searches have found already hints for the later-discovered Higgs boson in the form of significant excesses around 125 GeV. If `HiggsBounds` is now used to derive bounds on a Higgs boson with SM-like couplings and for example a mass of 128 GeV with a mass uncertainty of 4 GeV, the `HiggsBounds` algorithm chooses

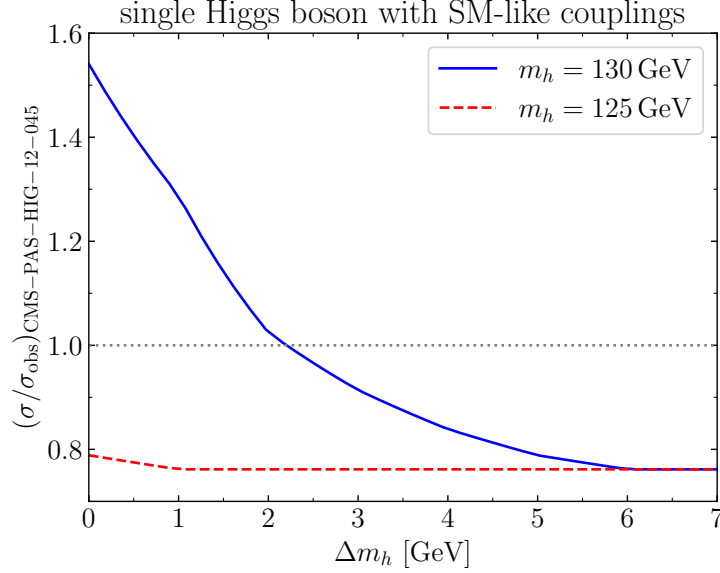


Figure 2: `HiggsBounds` observed ratio for the search of Ref. [37] derived for a single Higgs boson h with SM-like couplings as a function of its mass uncertainty. The results are shown for two different mass values: $m_h = 130$ GeV (blue) and $m_h = 125$ GeV (red).

to evaluate the pre-Higgs discovery limits at the mass value where the largest excess was observed, for instance at 125 GeV. As a result, the pre-Higgs discovery limits do not exclude this parameter point in accordance with the fact that the Higgs boson of the considered model can be identified with the Higgs boson that has been detected at 125 GeV (the extent to which the properties of the BSM scalar are compatible with the experimental results on the observed Higgs boson can be tested with `HiggsSignals`). If instead the mass value with the largest expected ratio were chosen, this could give rise to an evaluation of the limits at the lower or upper boundary of the mass interval leading to an exclusion of the respective parameter point.

Exemplary results derived using this prescription are shown in Fig. 2. In this Figure, we show the observed ratio for the search of Ref. [37] derived for a single Higgs boson h with SM-like couplings as a function of its mass uncertainty. For $m_h = 130$ GeV, we observe that the observed ratio decreases from ~ 1.55 to ~ 0.75 as we increase the mass uncertainty from zero to 7 GeV. If instead $m_h = 125$ GeV, the observed ratio stays essentially constant if increasing the mass uncertainty as expected.

2.2.4 Higgs pair production limits

While previous versions of `HiggsBounds` had already implemented some searches for resonant Higgs pair production, we significantly extended the scope of implemented searches with the new version, where the included experimental data now additionally comprises the limits of Refs. [38–45]. In addition, `HiggsBounds` now also implements an extensive list of searches for non-resonant Higgs pair production [38, 40, 44, 46–52].

`HiggsTools` offers no functionality to distinguish between resonant and non-resonant pair production. Therefore, the user has to find a self-defined criterion to decide which part of

Production channel	decay channel(s)	\sqrt{s} [TeV]	\mathcal{L} [fb $^{-1}$]	reference
$pp \rightarrow H^{\pm\pm} H^{\mp\mp}$	$H^{\pm\pm} \rightarrow \ell^{\pm} \ell^{\pm}$	8	19.7	[54]
$pp \rightarrow H^{\pm\pm} H^{\mp}$	$H^{\pm\pm} \rightarrow \ell^{\pm} \ell'^{\pm}, H^{\mp} \rightarrow \ell^{\mp} \nu_{\ell}$	8	19.7	[54]
$pp \rightarrow H^{\pm\pm} H^{\mp\mp}$	$H^{\pm\pm} \rightarrow e^{\pm} \tau^{\pm}, \mu^{\pm} \tau^{\pm}$	8	20.3	[55]
$pp \rightarrow H^{\pm\pm} H^{\mp\mp}$	$H^{\pm\pm} \rightarrow e^{\pm} e^{\pm}, e^{\pm} \mu^{\pm}, \mu^{\pm} \mu^{\pm}$	8	20.3	[56]
$pp \rightarrow H^{\pm\pm} H^{\mp\mp}$	$H^{\pm\pm} \rightarrow \ell^{\pm} \ell^{\pm}$	13	12.9	[57]
$pp \rightarrow H^{\pm\pm} H^{\mp}$	$H^{\pm\pm} \rightarrow \ell^{\pm} \ell'^{\pm}, H^{\mp} \rightarrow \ell^{\mp} \nu_{\ell}$	13	12.9	[57]
$pp \rightarrow H^{\pm\pm} H^{\mp\mp}$	$H^{\pm\pm} \rightarrow e^{\pm} e^{\pm}, e^{\pm} \mu^{\pm}, \mu^{\pm} \mu^{\pm}$	13	36	[58]
$pp \rightarrow H^{\pm\pm} H^{\mp\mp}$	$H^{\pm\pm} \rightarrow W^{\pm} W^{\pm}$	13	139	[59]
$pp \rightarrow H^{\pm\pm} H^{\mp}$	$H^{\pm\pm} \rightarrow W^{\pm} W^{\pm}, H^{\mp} \rightarrow W^{\mp} Z$	13	139	[59]

Table 2: Overview of implemented doubly charged Higgs searchers (with $\ell, \ell' = e, \mu, \tau$).

the considered parameter region should be confronted with resonant or with non-resonant pair-production limits (see e.g. Ref. [53]). Then, the input for resonant Higgs pair production can be set by specifying cross section values for pair decay processes and the input for non-resonant Higgs production can be set by providing appropriate values for pair production processes.

2.2.5 Doubly-charged Higgs bosons

As an additional new feature, **HiggsBounds** can now also check search limits for doubly-charged Higgs bosons. These appear in triplet or higher multiplet extensions of the SM Higgs sector. An overview of the implemented searches is given in Table 2. While most existing searches concentrate on leptonic final states, with the recent results presented in Ref. [59] also a search with bosonic final states is implemented.

2.3 HiggsSignals

Also **HiggsSignals** has been completely reimplemented in modern C++. The underlying approach is largely unchanged and has been described in detail in Ref. [9]. With the reimplementations in modern C++, the handling of the different measurement types (i.e., peak-centered observables, mass-centered observables, and STXS measurements) has been unified. At the moment, **HiggsSignals** implements 131 individual measurements.

As a new feature **HiggsSignals-3** now also contains the implementation of Higgs measurements which are not simple rate measurements but which can also depend on other model parameters. An example is the recent CMS $H \rightarrow \tau^+ \tau^-$ \mathcal{CP} analysis [60], which is part of the updated **HiggsSignals** dataset. This analysis is targeted at measuring the \mathcal{CP} structure of the tau-Yukawa coupling. The results are presented in dependence on the Higgs production via gluon fusion signal strength, the Higgs production via vector-boson fusion signal strength, and the \mathcal{CP} -violating phase ϕ_{τ} , defined via

$$\tan \phi_{\tau} = \frac{\tilde{c}_{\tau}}{c_{\tau}}, \quad (8)$$

where c_{τ} and \tilde{c}_{τ} are the coefficients of the \mathcal{CP} -even and \mathcal{CP} -odd tau-Yukawa coupling (multiplied by the SM tau-Yukawa coupling), respectively. The implementation of such lim-

its depending on the coupling structure of the Higgs boson has not been possible with `HiggsSignals-2` implying the need to externally evaluate the χ^2 . This strategy has e.g. been used for the results presented in Ref. [61]. The new `HiggsSignals` version allows to fully take such dependencies into account and therefore allows a straightforward implementation of results like the CMS $H \rightarrow \tau^+\tau^-$ \mathcal{CP} analysis [60].

3 C++, Python, and Mathematica interfaces

In this Section, we give an overview of the main functionality of the different program parts. The discussion will not mention (and explain) all available functions and options. Instead, it is aimed at introducing the program flow of `HiggsTools`. For a detailed list of all available functions and options, we refer to the online documentation available at

<https://higgsbounds.gitlab.io/higgstools>.

All shown code snippets are also distributed as parts of complete programs alongside the package.

3.1 Installation

`HiggsTools` is available at

<https://gitlab.com/higgsbounds/higgstools>.

It requires the following software packages:

- `gcc` (at least version 9) or `clang` (at least version 5),
- `CMake` (at least version 3.17),
- for the `Python` interface: `python` (at least version 3.5) and the corresponding development headers,
- for the `Mathematica` interface: `Wofram Mathematica`.

All other dependencies are compile-time only, and are automatically downloaded by `CMake`. The `HiggsTools` C++ can be built by running e.g.

```
mkdir build && cd build
cmake ..
make
```

within the `HiggsTools` directory.

To build the `Python` interface, type

```
pip install .
```

from within the `HiggsTools` folder (either before or after following the above steps).

To build the `Mathematica` executable, use

```
cmake -DHiggsTools_BUILD_MATHEMATICA_INTERFACE=ON ..
```

when building the C++ library. The `MHiggsTools` executable, which can be loaded from within `Mathematica`, can then be found in the `build/wstp` directory.

The collections of limits/measurements for `HiggsBounds` and `HiggsSignals` are available at <https://gitlab.com/higgsbounds/hbdataset> and <https://gitlab.com/higgsbounds/hsdataset>.

3.2 The C++ and Python interfaces

First, we explain how to run `HiggsTools` using the C++ and Python interfaces. The syntax of these interfaces is very similar.

The C++ libraries are loaded via

```
#include "Higgs/Bounds.hpp"
#include "Higgs/Predictions.hpp"
#include "Higgs/Signals.hpp"

namespace HP = Higgs::predictions;
```

where in the last line a purely optional abbreviation is introduced.

The `HiggsTools` Python package can e.g. be loaded via

```
import Higgs.predictions as HP
import Higgs.bounds as HB
import Higgs.signals as HS
```

where again some optional abbreviations are introduced.

3.2.1 User input via `HiggsPredictions`

As a first step, the user has to initialize the `HiggsPredictions` object e.g. by

```
auto pred = Higgs::Predictions{};
```

In Python, one can just write

```
pred = Higgs.Predictions()
```

This object can then be used to define all relevant scalar bosons via the `addParticle` function,

```
auto &h = pred.addParticle(HP::BsmParticle{"h", HP::ECharge::neutral,
                                          HP::CP::even});
```

or in Python via

```
h = pred.addParticle(HP.BsmParticle("h", "neutral", "even"))
```

The properties of the particles can then be defined e.g. by

```
h.setMass(1000);
```

or in Python via

```
h.setMass(1000)
```

Cross section values and partial decay widths can be given via

```
h.setCxn(HP::Collider::LHC13, HP::Production::ggH, 0.003)  
h.setDecayWidth(HP::Decay::tautau, 0.4)
```

or in Python via

```
h.setCxn("LHC13", "ggH", 0.003)  
h.setDecayWidth("tautau", 0.4)
```

where in the first line we set a cross section of 3 fb for h production via gluon fusion at the 13 TeV LHC. In the second line, we set a partial decay width of 400 MeV for the h decay into two tau leptons. Alternatively, also the total decay width and branching ratios can be set, e.g. via

```
h.setTotalWidth(0.4);  
h.setBr(HP::Decay::tautau, 1);
```

or in Python via

```
h.setTotalWidth(0.4)  
h.setBr("tautau", 1)
```

where in this example we set the total width to 400 MeV and the branching ratio into tau leptons to 100%.

As an alternative to providing explicit values for cross sections and decay widths (or branching ratios), the user can also refer to reference models and use the effective coupling input. For example, all couplings of the scalar h can be set to values twice as large as for the SM Higgs boson via

```
effC = HP::scaledSMlikeEffCouplings(2);  
HP::effectiveCouplingInput(h, effC);
```

or in Python via

```
effC = HP.scaledSMlikeEffCouplings(2)  
HP.effectiveCouplingInput(h, effC)
```


The cross sections and branching ratios of `h` will then be set automatically using this coupling input. One should note that after setting the effective couplings as given above, one cannot set an additional branching ratio by calling `h.setBr()`, as this would result in an error due to the fact that the sum of the branching ratios of `h` would exceed one. Instead, additional decay modes of the scalar can be defined by the user using the function `h.setDecayWidth()`, in which case internally all previously calculated branching ratios are automatically modified accordingly. We also note that, instead of a global rescaling factor, also all couplings can be set individually (see the example discussed in Sect. 4.1). Moreover, for the Higgs–fermion couplings, complex coupling values can be set corresponding to a \mathcal{CP} -even (real part) and a \mathcal{CP} -odd (imaginary part) Yukawa coupling.

3.2.2 Running HiggsBounds

As a first step, one has to initialize `HiggsBounds` by

```
const auto bounds = Higgs::Bounds("/Path/To/HBDataSet");
```

or in Python by

```
bounds = HB.Bounds("/Path/To/HBDataSet")
```

By this command, all limit files in the given folder are read-in and the `HiggsBounds` object is created. One can then use this object to check the bounds on a given `HiggsPredictions` object,

```
const auto resultHB = bounds(pred);
```

or in Python,

```
resultHB = bounds(pred)
```

The `result` object will then be either `True` or `False` depending on whether the chosen parameter point is allowed or not. More information can be extracted by typing

```
std::cout << resultHB << std::endl;
```

or in Python by typing

```
print(resultHB)
```

resulting in

```
HiggsBounds result: excluded
particle | obsRatio | expRatio | selected limit description
-----|-----|-----|-----
      h  |    1.676 |    0.774 | 2d likelihood {LHC13 [ggH>tautau],
              |          |          | LHC13 [bbH>tautau]} from 2002.12223
              |          |          | (ATLAS 139fb-1, M=(200, 2500))
```

as output for the example outlined above (not using the effective coupling input). Alternatively, a list of all selected or applied limits³ can be obtained via

```
resultHB.selectedLimits
```

or

```
resultHB.appliedLimits
```

in either C++ or Python.

3.2.3 Running HiggsSignals

In the same way as for HiggsBounds, the first step in order to use HiggsSignals is to initialize it by providing the path to the data set folder via

```
const auto signals = Higgs::Signals("/Path/To/HSDataset");
```

or in Python via

```
signals = HS.Signals("/Path/To/HSDataset")
```

The χ^2 analysis of HiggsSignals given a HiggsPredictions object as argument can then be invoked via

```
auto resultHS = signals(pred);
```

or in Python via

```
resultHS = signals(pred)
```

The return object is the total χ^2 value taking into account the whole data set.

It is also possible to perform the analysis individually for each measurement that is contained in the data set. For instance, in order to obtain the individual χ^2 values for all measurements separately, one can loop over the object `signals.measurements()` and apply `signals()` on each element,

```
for (const auto &m : signals.measurements()) {  
    std::cout << m.reference() << " " << m(pred) << std::endl;  
}
```

or in Python via

```
for m in signals.measurements():  
    print(f"{m.reference()}: {m(pred)}")
```

³All limits are applied to the model predictions. Out of these applied limits, the limit with the highest expected sensitivity is selected for each BSM scalar (see Section 2.2).

These code snippets return the reference numbers of the experimental measurements and the corresponding individual χ^2 values. Here, it should be noted that the sum of the χ^2 values will be larger than the total χ^2 value, because for obtaining the latter the correlations between the different measurements are taken into account.

3.3 Mathematica

As an alternative to the C++/Python interface, HiggsTools can also be used via Mathematica. As a consequence of the different structure of the Wolfram language, the syntax differs from the C++/Python interface.

The Mathematica executable can be loaded via

```
Install["/Path/To/MHiggsTools"];
```

This automatically initializes the HiggsPredictions, HiggsBounds, and HiggsSignals objects. Particles can then be added via

```
HPAddParticle["H", 1000, "neutral", "even"];
```

Their properties can be set e.g. via

```
HPSetCxn["H", "LHC13", "ggH", 0.003];  
  
HPSetDecayWidth["H", "tautau", 0.4];  
(* or *)  
HPSetTotalWidth["H", "LHC13", 0.4];  
HPSetBr["H", "tautau", 1];
```

Alternatively the effective coupling input can be used e.g. via

```
HPScaledSMlikeEffCouplings["H", 2];
```

HiggsBounds is initialized via

```
HBInitialize["/Path/To/HBDataSet"];
```

and run via

```
HBApplyBounds[]
```

The applied and selected limits can be assessed via

```
HBGetSelectedBounds[]  
HBGetAppliedBounds[]
```

Similarly, HiggsSignals is initialized via

```
HSInitialize["/Path/To/HSDataset"];
```

and run via

```
HSGetChisq[]
```

A list of individual χ^2 values can be obtained e.g. via

```
{reference /. #, HSGetChisqMeasurement[id /. #]} & /@ HSListMeasurements[]
```

where `HSListMeasurements[]` returns a list of all loaded measurements.

4 Examples

In this Section, we present some examples using the different components of `HiggsTools` to derive non-trivial constraints on BSM models with an extended or modified Higgs sector.

All these examples use the `Python` interface. Complete code examples (using also the `C++` and `Mathematica` interfaces) are distributed alongside the package. For the `Python` and `Mathematica` scripts also the necessary plotting commands are included.

4.1 Constraining the charm Yukawa coupling with HiggsSignals

While the couplings of h_{125} to the third-generation fermions have been measured at the LHC at the level of 10% [62, 63], the couplings to the first- and second-generation fermions are only weakly constrained so far. It is therefore worthwhile to derive indirect constraints on these couplings via the signal-rate measurements of h_{125} . We will show here how `HiggsSignals` can be utilized to set bounds on the coupling of h_{125} to charm quarks under the assumption that all other couplings of h_{125} are SM-like. This example will also demonstrate the importance of choosing the correct SM reference model for the cross sections of the Higgs boson for the case in which the effective-coupling input is used.

A state that has the same couplings as a SM Higgs boson except for the charm-quark coupling can be defined in `HiggsSignals` in the following way,⁴

```
cpls = Higgs.predictions.NeutralEffectiveCouplings()
cpls.tt = 1
cpls.bb = 1
cpls.tautau = 1
cpls.ss = 1
cpls.mumu = 1
cpls.gg = 1
cpls.ZZ = 1
cpls.WW = 1
cpls.gamgam = 1
cpls.Zgam = 1
```

⁴The couplings to first generation fermions are set to their SM values by default.

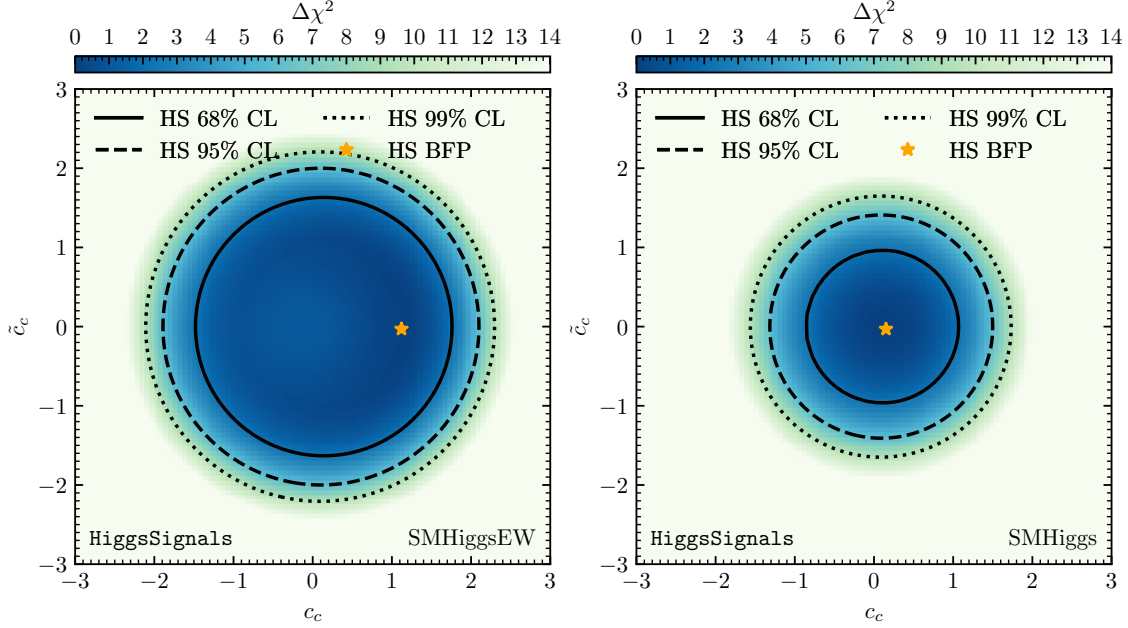


Figure 3: Constraints on the modified coupling of h_{125} to charm quarks in the plane of the coupling modifiers c_c and \tilde{c}_c . In the left plot the reference model `SMHiggsEW` was used for the `HiggsSignals` analysis, whereas the right plot shows the results using the reference model `SMHiggs`. The orange star in each plot indicates the best fit point of the `HiggsSignals` analysis. The SM values are $c_c = 1$ and $\tilde{c}_c = 0$

```
cpls.cc = 0.9 + 1j * 0.1
Higgs.predictions.effectiveCouplingInput(
    h,
    cpls,
    reference=HP.ReferenceModel.SMHiggsEW)
```

As an example, we set here the \mathcal{CP} -even Yukawa coupling to $c_c = 0.9$ and the \mathcal{CP} -odd Yukawa coupling to $\tilde{c}_c = 0.1$ (times the SM charm-Yukawa coupling), where the latter has to be given as the imaginary component of `cpls.cc`. Note also that we chose here `SMHiggsEW` as the reference model in order to utilize the predictions for the cross section of the Higgs boson that include N3LO QCD corrections in the heavy top-quark limit and NLO electroweak corrections.

Following the discussion in Section 3.2.3, the χ^2 -analysis of `HiggsSignals` for the coupling configuration as defined above can now be executed via

```
Chisq = signals(pred)
```

In the left plot of Fig. 3, we show the result of the analysis for a scan over both c_c and \tilde{c}_c . The color coding indicates the difference of the χ^2 -values with respect to the best-fit point. As expected, the lowest values of $\Delta\chi^2$ are found for $c_c^2 + \tilde{c}_c^2 = 1$, the region that includes the SM prediction $c_c = 1$ and $\tilde{c}_c = 0$. The result of `HiggsSignals` is different if instead of `SMHiggsEW` the reference model `SMHiggs` is chosen in the call of `effectiveCouplingInput()`. The χ^2

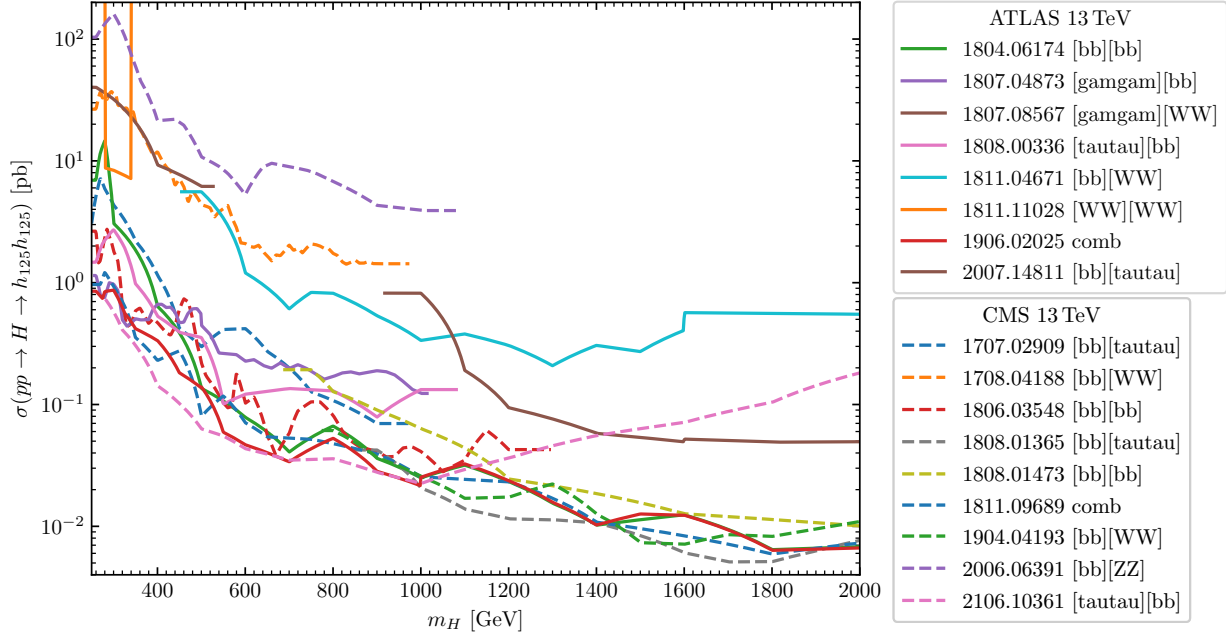


Figure 4: 95% confidence-level cross section limits on the process $pp \rightarrow H \rightarrow h_{125}h_{125}$ from the experimental searches in various final states. The dashed lines show results from the CMS collaboration, whereas the solid lines show results from the ATLAS collaboration.

contribution for the option **SMHiggs** is shown in the right plot of Fig. 3. One can see that in this case **HiggsSignals** finds as the best-fit point the point with vanishing couplings, and the SM would be disfavoured at a confidence level of about 1σ . The difference between the two plots arises from the fact that the reference model **SMHiggs** uses the QCD NNLO predictions for the reference cross section, whereas **SMHiggsEW** uses the N3LO predictions in the heavy top-quark limit. The comparison between the two plots shows that this kind of analysis is sensitive to QCD corrections beyond the NNLO level in the employed cross section predictions. This example illustrates the importance of choosing the correct reference model. The option **SMHiggs** is the preferred choice for particles that have a mass comparable to the top-quark mass or larger, whereas for a particle state at 125 GeV one should use **SMHiggsEW** in order to include the QCD corrections beyond the NNLO.

4.2 Sensitivity comparison of resonant h_{125} -pair production with HiggsBounds

As already discussed in Section 2.2.4, **HiggsBounds-6** contains a substantially extended scope of experimental results from searches for resonant pair production of h_{125} . In order to illustrate the full extent of the implemented searches, we show in Fig. 4 the limits on the cross section $\sigma(pp \rightarrow H \rightarrow h_{125}h_{125})$ for the different searches as they are currently implemented in the new version of **HiggsBounds**. We also show the combined result of both the CMS collaboration (red solid line) and the ATLAS collaboration (blue dashed line) in which the data of various different final states have been included. As discussed in Section 2.2.4, a large part of the experimental searches shown in Fig. 4 were not yet implemented in the

previous `HiggsBounds` version. As a result, the new version presented here can give rise to substantially stronger bounds for models in which resonant h_{125} -pair production is relevant.

In order to obtain the cross-section limits shown in Fig. 4 from their implementation in `HiggsBounds`, one can define a SM-like Higgs boson h with a mass of 125 GeV and a heavy state H with varying mass, and which has a gluon fusion production cross section of 1 pb and a branching ratio of 1 into h_{125} -pairs:

```
h = pred.addParticle(HP.NeutralScalar("h", cp="even"))
H = pred.addParticle(HP.NeutralScalar("H"))

h.setMass(125.09)
HP.effectiveCouplingInput(h, HP.smLikeEffCouplings)
H.setDecayWidth("h", "h", 1)
H.setCxn("LHC13", "ggH", 1)
```

Here we defined only one partial width for the heavy scalar H corresponding to the decay $H \rightarrow h_{125}h_{125}$. Consequently, independently of the value chosen for this decay width, the corresponding branching ratio is equal to 1. Afterwards, one can call the `HiggsBounds` check for different values of the mass of the heavy state and read off the observed ratio for all applied limits that belong to the class of resonant h_{125} pair production:

```
masses = np.arange(250, 2001, 10)
results = {}
for m in masses:
    H.setMass(m)
    results[m] = [
        1 for l in bounds(pred).appliedLimits if
            "H" in l.contributingParticles()]
```

The observed ratio is defined as the ratio of predicted cross section and the experimental limit at the 95% confidence level. Since we set the cross section for the process to 1pb independently of the mass of the heavy state, the experimental limit for each mass can thus be obtained by simply calculating the inverse of the observed ratio:

```
limits = list({a.limit() for res in results.values() for a in res})
data = {}
for lim in limits:
    data[lim.id()] = {
        m: 1 / x.obsRatio() for m, res in results.items() for
            x in res if x.limit() == lim}
```

Here the object `data` contains the information shown in Fig. 4: for each applied experimental search it saves the experimental limit as a function of the mass of the scalar H .

4.3 Constraining the width of the h_{125} Higgs boson with HiggsSignals

The SM prediction for the total width of the Higgs boson at 125 GeV is $\Gamma_{h_{125}}^{\text{SM}} \sim 4$ MeV. At a hadron collider, such as the LHC, there is no direct access to the total width of h_{125} under the assumption that $\Gamma_{h_{125}} \ll 1$ GeV.⁵ As a result, there may be room for new physics that gives rise to modifications of the total width of h_{125} while maintaining values of the measured signal rates of h_{125} close to the SM predictions. The simplest example of such a scenario is a model in which the properties of h_{125} are modified compared to the SM in a twofold way: First, one can assume that there is an additional decay mode of h_{125} that is undetected.⁶ The branching ratio for this new-physics decay mode is denoted $\text{BR}(h_{125} \rightarrow \text{NP})$ in the following, and it gives rise to an enhancement of $\Gamma_{h_{125}}$. In addition, in order to compensate for the suppression of the measured signal rates due to the additional $h \rightarrow \text{NP}$ decay mode, one can assume that the couplings of h_{125} to SM particles are enhanced compared to the SM predictions by an overall factor $c_{\text{eff}} > 1$.

With `HiggsSignals` it is very easy to confront this BSM scenario with the experimental constraints from the LHC. For instance, an enhancement of the couplings by the factor $c_{\text{eff}} = 2$ can be set (as already discussed in Section 3.2.1) with:

```
ceff = 2
cpl = Higgs.predictions.scaledSMlikeEffCouplings(ceff)
Higgs.predictions.effectiveCouplingInput(
    h,
    cpl,
    reference=Higgs.predictions.ReferenceModel.SMHiggsEW)
```

Calling `effectiveCouplingInput()` automatically invokes the calculation of the partial widths for the decays into SM particles. At the same time, the total width is set to be equal to the sum of all these partial widths. In order to define, for example, $\text{BR}(h_{125} \rightarrow \text{NP}) = 0.4$ one can use the function `setDecayWidth()`.⁷

```
totalWidthbefore = h.totalWidth()
branchingRatioNP = 0.4
partialWidthNP = branchingRatioNP * totalWidthbefore / \
    (1 - branchingRatioNP)
h.setDecayWidth('NP', partialWidthNP)
```

The argument 'NP' can be interchanged with any string expression that does not correspond to any of the particle names defined by the user. Now the input is complete and one can

⁵See Ref. [64] for an indirect measurement of $\Gamma_{h_{125}}$ at the MeV-level via off-shell effects in Higgs boson production. This indirect determination of $\Gamma_{h_{125}}$ relies, however, on several assumptions that are not necessarily fulfilled in BSM scenarios.

⁶We note here the distinction between an “undetected” decay mode, which cannot be distinguished from the background, and an “invisible” decay mode. The latter may very well be detectable because of its characteristic signature of missing energy/momentum in the event.

⁷One cannot use `setBR()` at this point, since this would give rise to a runtime error due to the sum of all branching ratios being larger than 1.

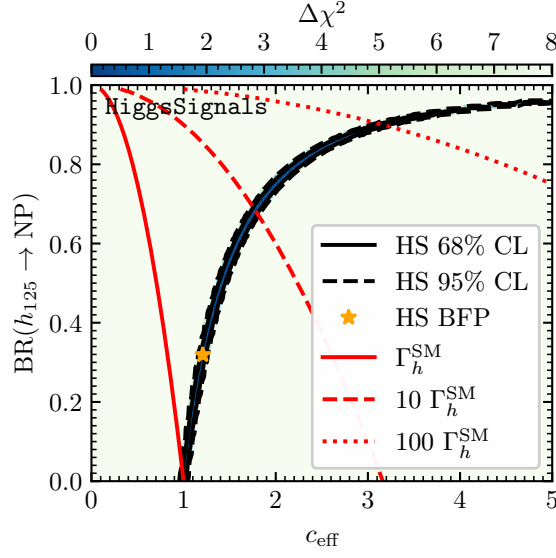


Figure 5: χ^2 result according to the HiggsSignals analysis for the scenario discussed in Sect. 4.3. The color coding indicates the value of $\Delta\chi^2$, which is defined relative to the best-fit χ^2 -value. The solid and dashed black lines indicate the allowed regions at the 68% and the 95% confidence level, respectively. The orange star indicates the best-fit point. The solid, dashed and dotted red lines indicate where the total width of the Higgs boson has a value of 1, 10 and 100 times the SM prediction, respectively.

call the HiggsSignals analysis:

```
Chisq = signals(pred)
```

Here the objects `pred` and `signals` have to be initialized as explained in Section 3.2.1 and Section 3.2.3, respectively.

Fig. 5 shows the result of the χ^2 analyses when scanning over $0 \leq c_{\text{eff}} \leq 5$ and $0 \leq \text{BR}(h_{125} \rightarrow \text{NP}) \leq 1$. We find a narrow band in the plane of c_{eff} and $\text{BR}(h_{125} \rightarrow \text{NP})$ with low values of $\Delta\chi^2 < 5.99$, where $\Delta\chi^2 = \chi^2 - \chi_{\text{best}}^2$, and $\chi_{\text{best}}^2 = \min(\chi^2)$ denotes the best-fit value. We also indicate with red lines the contours for which the total width of h_{125} is equal to 1, 10 or 100 times the SM prediction. The SM point in this plot corresponds to $c_{\text{eff}} = 1$ and $\text{BR}(h_{125} \rightarrow \text{NP}) = 0$. It has a $\Delta\chi^2 = 0.06$ value relative to the best-fit point that is located at $c_{\text{eff}} = 1.21$ and $\text{BR}(h_{125} \rightarrow \text{NP}) = 0.32$. As mentioned above, HiggsSignals does not compare to the indirect determinations of the total width via off-shell effects, since these analyses are not applicable in a generic fashion to BSM scenarios. For instance, in this example there is a new-physics decay mode for the Higgs boson whose impact on the off-shell effects would have to be taken into account. In fact, currently HiggsSignals does not contain any direct constraint on the total width of h_{125} , such that the region with acceptable values of $\Delta\chi^2$ would extend for $c_{\text{eff}} > 5$ until infinity, asymptotically approaching $\text{BR}(h_{125} \rightarrow \text{NP}) = 1$. Of course, for total width values in the GeV range the direct search limits from the LHC would apply. Furthermore, the relatively large values of the Higgs couplings that would be needed in this example in order to accommodate sizable values of $\text{BR}(h_{125} \rightarrow \text{NP})$ could also be tested by other experimental constraints.

4.4 Constraining the 2HDM

One of the most studied BSM scenarios is the Two-Higgs doublet model (2HDM), which extends the SM by a second SU(2) doublet field [65, 66] (see Ref. [67] for a review). Assuming \mathcal{CP} conservation, the Higgs sector of the 2HDM consists of two \mathcal{CP} -even states h and H , where here we assume that h plays the role of the discovered Higgs boson at $m_h = 125$ GeV, a \mathcal{CP} -odd state A , and two charged Higgs bosons H^\pm , where m_H , m_A and m_{H^\pm} are the masses of the BSM Higgs bosons.

In order to avoid flavor-changing neutral currents, a softly broken Z_2 symmetry can be introduced, under which one of the Higgs doublets changes the sign, and where m_{12}^2 denotes the Z_2 -breaking mass parameter. There are four different ways of assigning charges of the fermions under the Z_2 symmetry, giving rise to the four different Yukawa types of the 2HDM. Each type features a different dependence of the couplings of the Higgs bosons on the angles α and $\tan\beta$, where α is the mixing angle in the \mathcal{CP} -even sector, and $\tan\beta$ is defined as the ratio of the vevs of the \mathcal{CP} -even states.

In Fig. 6 we show the constraints in the $\cos(\alpha - \beta)$ – $\tan\beta$ parameter plane for the four Yukawa types as they result from the χ^2 -fit of `HiggsSignals` and from the `HiggsBounds` analysis.⁸ The result for $\Delta\chi^2 = \chi^2 - \chi_{\text{best}}^2$, where χ_{best}^2 denotes the best-fit value, can be obtained by making use of the effective coupling input format, based on the cross sections and branching ratios of h that can be determined with the help of the `HiggsPredictions` subpackage (see Section 2.1 for details). The only model information the user has to provide are the effective couplings as functions of α and β .⁹ For instance, in order to define the couplings of h to the third-generation fermions in the type II 2HDM one can write:

```
h = pred.addParticle(Higgs.predictions.NeutralScalar("h"))
cpls_h = Higgs.predictions.NeutralEffectiveCouplings()
cpls_h.tt = cos(alpha) / sin(beta)
cpls_h.bb = -sin(alpha) / cos(beta)
cpls_h.tautau = -sin(alpha) / cos(beta)
...
Higgs.predictions.effectiveCouplingInput(
    h,
    cpls_h,
    reference=Higgs.predictions.ReferenceModel.SMHiggsEW)
```

The effective couplings to the vector bosons and the remaining fermions can be set in the same way as before calling `effectiveCouplingsInput()`. When all effective couplings have been set, the `HiggsSignals` χ^2 -result is obtained via:

```
Chisq = signals(pred)
```

It can be observed in Fig. 6 that for the types II, III and IV the best-fit point regarding `HiggsSignals` (orange star) is found close to the alignment limit, $\cos(\alpha - \beta) = 0$, in which

⁸A recent detailed analysis of this kind can be found in Ref. [68].

⁹We make the assumption here that since $m_H = m_A = m_{H^\pm} \gg m_h$ the impact of the heavy states H, A and H^\pm on the loop-induced couplings is negligible.

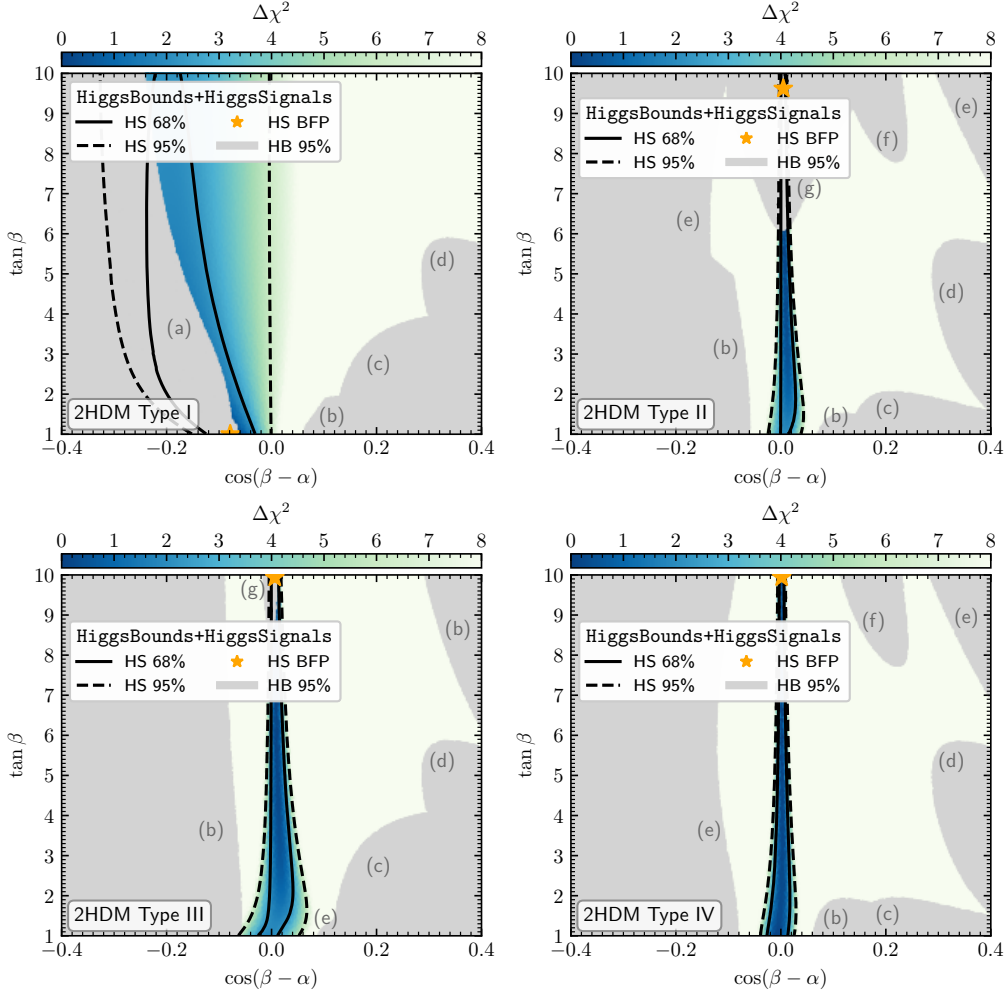


Figure 6: Constraints in the plane of the parameters $\cos(\beta - \alpha)$ and $\tan\beta$ in the four Yukawa types of the 2HDM for $m_H = m_A = m_{H^\pm} = \sqrt{m_{12}^2/(\sin\beta\cos\beta)} = 800$ GeV. The color coding indicates the value of $\Delta\chi^2$ obtained with **HiggsSignals**. The best-fit point with $\Delta\chi^2 = 0$ is indicated with an orange star in each plot. The gray regions are excluded based on the **HiggsBounds** result. The gray letters indicate the experimental search responsible for the corresponding exclusion limit. The details of the searches are specified in the text.

the properties of h in the 2HDM resemble the ones of a SM Higgs boson. For the Yukawa type I we find the smallest values of $\Delta\chi^2$ for slightly negative values of $\cos(\beta - \alpha)$, which is in agreement with the ATLAS result shown in Fig. 20 of Ref. [69]. With the new version of **HiggsSignals** it is very easy to identify the experimental measurement that gives rise to a change of χ^2 in a certain parameter region of a model. In the considered example, for instance for the type I, one can use **HiggsSignals** for two neighbouring parameter points at $\tan\beta = 1, \cos(\alpha - \beta) = 0$ and at $\tan\beta = 1, \cos(\alpha - \beta) = -0.1$ in order to obtain the individual χ^2 -values for each implemented measurement by typing (see Section 3.2.3 for details):

```
AllChisq1 = {m.reference(): m(pred1) for m in signals.measurements()}
AllChisq2 = {m.reference(): m(pred2) for m in signals.measurements()}
DeltaChisq = {k: AllChisq2[k] - AllChisq1[k] for k in AllChisq1}
```

Here `pred1` and `pred2` are the `Higgs.Predictions` objects for the two parameter points that have to be created previously according to the instructions above. In the third line we create a dictionary that contains the differences of the χ^2 -values for each experimental measurement. In this example we find that the increase of $\Delta\chi^2$ in the alignment limit of type I is mainly driven by the results of Refs. [60, 70, 71] which slightly disfavor the alignment limit at the level of about 2σ each (see also the discussion in Ref. [72]).

In addition to $\Delta\chi^2$, the plots in Fig. 6 also indicate in gray the parameter regions that are excluded according to the `HiggsBounds` analysis. For the considered example, the effective coupling input is not sufficient for calculating the branching ratios for the BSM states.¹⁰ In order to perform this analysis we therefore calculated the cross sections and branching ratios with the help of the external software packages `HDECAY` [11, 12, 73] and `SuSHi` [16, 17] (both called via `ScannerS` [74]). The predictions for the cross sections and branching ratios were then provided directly as input to `HiggsBounds`. This can be done with the following lines of code, here as an example for the \mathcal{CP} -odd Higgs boson A :

```
ACP = HP.CP(-1)
A = pred.addParticle(Higgs.predictions.NeutralScalar("A", ACP))
A.setMass(...)
A.setTotalWidth(...)
A.setBr('tt', ...)
...
A.setBr('Z', 'h', ...)
A.setCxn('LHC13', 'ggH', ...)
A.setCxn('LHC13', 'bbH', ...)
```

Here the ellipsis in the sixth line indicates additional definitions of branching ratios, whereas the ellipsis in the function arguments represents the numerical values the user has to provide in each case. When the branching ratios and cross sections of A , H and H^\pm have been set, the `HiggsBounds` analysis is executed by doing:

```
res = bounds(pred)
```

The desired information of the analysis, for instance the most sensitive channel selected by `HiggsBounds` for the state A , can be obtained with:

```
res.selectedLimits['A']
```

The corresponding values for the ratios of predicted cross section divided by expected or observed cross-section limit can be extracted with:

¹⁰The effective coupling input cannot be used for the charged Higgs boson. Moreover, the effects of the charged Higgs boson on the Higgs to di-photon branching ratios are not calculated by `HiggsPredictions`.

```
res.selectedLimits['A'].expRatio()
res.selectedLimits['A'].obsRatio()
```

The information about the other Higgs bosons can be obtained accordingly. The gray regions in the plots in Fig. 6 are defined by the condition that the `obsratio` for one of the Higgs bosons is larger than 1. The selected channels responsible for the different excluded regions are the following:

- (a) CMS: $pp \rightarrow \phi \rightarrow h_{125}h_{125} \rightarrow bb\gamma\gamma, b\bar{b}\tau\tau, bbbb, bbVV$ [49],
- (b) CMS: $pp \rightarrow \phi_1 \rightarrow h_{125}\phi_2 \rightarrow b\bar{b}\tau\tau$ [43],
- (c) CMS: $pp \rightarrow \phi \rightarrow Zh_{125} \rightarrow Zbb$ [31],
- (d) ATLAS: $pp \rightarrow \phi \rightarrow WW, ZZ, WZ$ [75],
- (e) ATLAS: $pp \rightarrow \phi \rightarrow h_{125}h_{125} \rightarrow bbbb$ [76],
- (f) ATLAS: $pp \rightarrow \phi \rightarrow VV, Vh_{125}$ [77],
- (g) ATLAS: $pp \rightarrow \phi \rightarrow \tau\tau$ [78],

where the letters in Fig. 6 indicate which limit excludes which parameter region.

5 Conclusions

We have presented new versions of the public computer programs `HiggsBounds` and `HiggsSignals`. The program `HiggsBounds` tests general BSM models against exclusion limits from LEP and LHC Higgs searches (the limits from Tevatron searches have become less relevant compared to the LHC results and are no longer used). `HiggsSignals` confronts the predictions of arbitrary BSM models with the measured mass and rates of the Higgs boson that has been detected at about 125 GeV. The new versions, `HiggsBounds-6` and `HiggsSignals-3`, now use a common interface for the predictions of the various Higgs production and decay rates, provided by the new code `HiggsPredictions-1`. The complete suite of codes is provided within the new overarching code `HiggsTools-1`.

The description of `HiggsBounds-6` and `HiggsSignals-3`, together with the new code `HiggsPredictions-1`, provided in the present paper has focused on the improvements of the functionality and applicability of the programs with respect to the previous versions as given in Ref. [6] and [9] for `HiggsBounds` and `HiggsSignals`, respectively. The new code `HiggsPredictions`, which formerly was partly contained in `HiggsBounds`, facilitates the definition of the physical model. The user has to specify the scalar content of the model under consideration: the properties of each scalar of the model, including the mass, total width, charge, \mathcal{CP} character and the rates for all relevant production and decay channels. These properties can be set by the user directly, or alternatively via effective couplings. Concerning the latter option updated tabulated cross sections and branching ratios are included that are then rescaled using the effective coupling input.

Concerning `HiggsBounds`, the implemented limits are now classified into six different types, which facilitates the inclusion of new experimental data. These six types comprise (i) limits for a certain Higgs production and decay chain, (ii) the same as (i), but with a width dependent limit, (iii) the same as (i), but including a longer (Higgs) decay chain, (iv) limits on Higgs production with a di-Higgs pair decay mode, (v) limits on di-Higgs production and decay, (vi) likelihood limits. Also, the algorithm of particle clustering, relevant if several scalars can contribute to a specific limit, has been updated and improved. The set of di-Higgs search channels has been newly implemented (previously only a subset had been considered), as well as limits from searches for doubly charged Higgs bosons. The main update for `HiggsSignals` is the extension of the functionality to allow the implementation of Higgs measurements which are not simple rate measurements but which can also depend on other model parameters. This feature has been used in particular for the inclusion of the dedicated \mathcal{CP} analysis by CMS for the decay to $\tau^+\tau^-$, which targets the measurement of the \mathcal{CP} structure of the Higgs coupling to tau leptons. In our description of the codes we have also included detailed information on the C++, Python and Mathematica interfaces.

We have furthermore discussed in this paper several physics examples with a focus on demonstrating the new functionalities that are provided by `HiggsTools`, together with examples for the commands that have been used to obtain these example applications. The first example concerns constraints on the charm Yukawa coupling that have been obtained with `HiggsSignals`. It was demonstrated that the application of the correct Higgs-boson cross-section prediction is crucial to obtain reliable bounds on this Yukawa coupling. In the second physics example the sensitivity of several resonant h_{125} -pair production channels that are implemented in `HiggsBounds` has been compared. This example demonstrates the effects of the largely extended sample of di-Higgs search limits that are now included into `HiggsBounds`. In the third example, updating the previous analysis of Ref. [79] with the latest signal rates that are implemented in `HiggsSignals`, a scenario was considered where the total width of the Higgs boson at 125 GeV is enlarged by an undetected decay mode, while the effects of the enlarged width in the signal strength measurements are compensated by a universal scaling if the Higgs-boson couplings. In a final physics example we have demonstrated the combined and complementary power of `HiggsBounds` and `HiggsSignals`, with the 2HDM as a showcase. In the four Yukawa types of the 2HDM we analyzed the current status of the limits from direct searches (via `HiggsBounds`) and from the Higgs-boson rate measurements (via `HiggsSignals`) in dependence on the mixing angles, where all heavy Higgs-boson masses were set to 800 GeV. We showed that for all four Yukawa types significant BSM effects are allowed at the current level of accuracy, where in type I potentially the largest effects can occur.

The code `HiggsTools-1`, containing `HiggsPredictions-1`, `HiggsBounds-6` and `HiggsSignals-3`, is available via

<https://gitlab.com/higgsbounds/higgstools>.

Acknowledgements

The authors thank Philip Bechtle, Oliver Brein, Daniel Dercks, Oscar Stål, Tim Stefaniak, and Karina Williams for collaboration on earlier versions of `HiggsBounds` and `HiggsSignals`.

T.B., C.L., S.P. and G.W. acknowledge support by the Deutsche Forschungsgemeinschaft (DFG, German Research Foundation) under Germany's Excellence Strategy – EXC 2121 “Quantum Universe” – 390833306. This work has been partially funded by the Deutsche Forschungsgemeinschaft (DFG, German Research Foundation) - 491245950. The work of S.H. has received financial support from the grant PID2019-110058GB-C21 funded by MCIN/AEI/10.13039/501100011033 and by “ERDF A way of making Europe”. MEINCOP Spain under contract PID2019-110058GB-C21 and in part by the grant IFT Centro de Excelencia Severo Ochoa CEX2020-001007-S funded by MCIN/AEI/10.13039/501100011033.

References

- [1] ATLAS, “Observation of a new particle in the search for the Standard Model Higgs boson with the ATLAS detector at the LHC”, *Phys. Lett. B* **716** (2012) 1, [1207.7214](#).
- [2] CMS, “Observation of a New Boson at a Mass of 125 GeV with the CMS Experiment at the LHC”, *Phys. Lett. B* **716** (2012) 30, [1207.7235](#).
- [3] P. Bechtle et al., “HiggsBounds: Confronting Arbitrary Higgs Sectors with Exclusion Bounds from LEP and the Tevatron”, *Comput. Phys. Commun.* **181** (2010) 138, [0811.4169](#).
- [4] P. Bechtle et al., “HiggsBounds 2.0.0: Confronting Neutral and Charged Higgs Sector Predictions with Exclusion Bounds from LEP and the Tevatron”, *Comput. Phys. Commun.* **182** (2011) 2605, [1102.1898](#).
- [5] P. Bechtle et al., “HiggsBounds – 4: Improved Tests of Extended Higgs Sectors against Exclusion Bounds from LEP, the Tevatron and the LHC”, *Eur. Phys. J. C* **74** (2014) 2693, [1311.0055](#).
- [6] P. Bechtle et al., “HiggsBounds-5: Testing Higgs Sectors in the LHC 13 TeV Era”, *Eur. Phys. J. C* **80** (2020) 1211, [2006.06007](#).
- [7] H. Bahl et al., “Testing Exotic Scalars with HiggsBounds”, (2021), [2109.10366](#).
- [8] P. Bechtle et al., “*HiggsSignals*: Confronting arbitrary Higgs sectors with measurements at the Tevatron and the LHC”, *Eur. Phys. J. C* **74** (2014) 2711, [1305.1933](#).
- [9] P. Bechtle et al., “HiggsSignals-2: Probing new physics with precision Higgs measurements in the LHC 13 TeV era”, *Eur. Phys. J. C* **81** (2021) 145, [2012.09197](#).
- [10] LHC Higgs Cross Section Working Group, “Handbook of LHC Higgs Cross Sections: 4. Deciphering the Nature of the Higgs Sector”, *2/2017* (2016), [1610.07922](#).
- [11] A. Djouadi, J. Kalinowski, and M. Spira, “HDECAY: A Program for Higgs boson decays in the standard model and its supersymmetric extension”, *Comput. Phys. Commun.* **108** (1998) 56, [hep-ph/9704448](#).
- [12] A. Djouadi et al., “HDECAY: Twenty++ years after”, *Comput. Phys. Commun.* **238** (2019) 214, [1801.09506](#).
- [13] C. Degrande et al., “Heavy charged Higgs boson production at the LHC”, *JHEP* **10** (2015) 145, [1507.02549](#).
- [14] C. Degrande et al., “Accurate predictions for charged Higgs production: Closing the $m_{H^\pm} \sim m_t$ window”, *Phys. Lett. B* **772** (2017) 87, [1607.05291](#).
- [15] H. Bahl, T. Stefaniak, and J. Wittbrodt, “The forgotten channels: charged Higgs boson decays to a W^\pm and a non-SM-like Higgs boson”, *JHEP* **06** (2021) 183, [2103.07484](#).
- [16] R. V. Harlander, S. Liebler, and H. Mantler, “SusHi: A program for the calculation of Higgs production in gluon fusion and bottom-quark annihilation in the Standard Model and the MSSM”, *Comput. Phys. Commun.* **184** (2013) 1605, [1212.3249](#).
- [17] R. V. Harlander, S. Liebler, and H. Mantler, “SusHi Bento: Beyond NNLO and the heavy-top limit”, *Comput. Phys. Commun.* **212** (2017) 239, [1605.03190](#).

- [18] M. Ciccolini, A. Denner, and S. Dittmaier, “Strong and electroweak corrections to the production of Higgs + 2jets via weak interactions at the LHC”, *Phys. Rev. Lett.* **99** (2007) 161803, [0707.0381](#).
- [19] M. Ciccolini, A. Denner, and S. Dittmaier, “Electroweak and QCD corrections to Higgs production via vector-boson fusion at the LHC”, *Phys. Rev. D* **77** (2008) 013002, [0710.4749](#).
- [20] A. Denner et al., “Electroweak corrections to Higgs-strahlung off W/Z bosons at the Tevatron and the LHC with HAWK”, *JHEP* **03** (2012) 075, [1112.5142](#).
- [21] A. Denner et al., “HAWK 2.0: A Monte Carlo program for Higgs production in vector-boson fusion and Higgs strahlung at hadron colliders”, *Comput. Phys. Commun.* **195** (2015) 161, [1412.5390](#).
- [22] J. Alwall et al., “The automated computation of tree-level and next-to-leading order differential cross sections, and their matching to parton shower simulations”, *JHEP* **07** (2014) 079, [1405.0301](#).
- [23] A. Martin et al., “Parton distributions for the LHC”, *Eur. Phys. J. C* **63** (2009) 189, [0901.0002](#).
- [24] M. Whalley, D. Bourilkov, and R. Group, “The Les Houches accord PDFs (LHAPDF) and LHAGLUE”, in: *HERA and the LHC: A Workshop on the implications of HERA for LHC physics. Proceedings, Part B*, 2005 575, [hep-ph/0508110](#).
- [25] O. Brein, R. V. Harlander, and T. J. E. Zirke, “vh@nnlo - Higgs Strahlung at hadron colliders”, *Comput. Phys. Commun.* **184** (2013) 998, [1210.5347](#).
- [26] R. V. Harlander et al., “vh@nnlo-v2: New physics in Higgs Strahlung”, *JHEP* **05** (2018) 089, [1802.04817](#).
- [27] H. Bahl et al., “Indirect \mathcal{CP} probes of the Higgs-top-quark interaction: current LHC constraints and future opportunities”, *JHEP* **11** (2020) 127, [2007.08542](#).
- [28] *HiggsTools online documentation (limit implementation)*, <https://higgsbounds.gitlab.io/higgstools/Datafile.html>.
- [29] ATLAS, “Search for heavy neutral Higgs bosons produced in association with b -quarks and decaying into b -quarks at $\sqrt{s} = 13$ TeV with the ATLAS detector”, *Phys. Rev. D* **102** (2020) 032004, [1907.02749](#).
- [30] CMS, “Search for a new scalar resonance decaying to a pair of Z bosons in proton-proton collisions at $\sqrt{s} = 13$ TeV”, *JHEP* **06** (2018) 127, [1804.01939](#).
- [31] CMS, “Search for a heavy pseudoscalar boson decaying to a Z and a Higgs boson at $\sqrt{s} = 13$ TeV”, *Eur. Phys. J. C* **79** (2019) 564, [1903.00941](#).
- [32] CMS, “Search for Higgs boson pair production in events with two bottom quarks and two tau leptons in proton–proton collisions at $\sqrt{s} = 13$ TeV”, *Phys. Lett. B* **778** (2018) 101, [1707.02909](#).
- [33] ALEPH, DELPHI, L3, OPAL, LEP Working Group for Higgs Boson Searches, “Search for neutral MSSM Higgs bosons at LEP”, *Eur. Phys. J. C* **47** (2006) 547, [hep-ex/0602042](#).

- [34] CMS, “Search for additional neutral MSSM Higgs bosons in the $\tau\tau$ final state in proton-proton collisions at $\sqrt{s} = 13$ TeV”, *JHEP* **09** (2018) 007, [1803.06553](#).
- [35] P. Bechtle et al., “Applying Exclusion Likelihoods from LHC Searches to Extended Higgs Sectors”, *Eur. Phys. J. C* **75** (2015) 421, [1507.06706](#).
- [36] P. Slavich et al., “Higgs-mass predictions in the MSSM and beyond”, *Eur. Phys. J. C* **81** (2021) 450, ed. by P. Slavich and S. Heinemeyer, [2012.15629](#).
- [37] CMS, “Combination of standard model Higgs boson searches and measurements of the properties of the new boson with a mass near 125 GeV”, (2012), CMS-PAS-HIG-12-045.
- [38] CMS, “Search for resonant and nonresonant Higgs boson pair production in the $b\bar{b}\ell\nu\ell\nu$ final state in proton-proton collisions at $\sqrt{s} = 13$ TeV”, *JHEP* **01** (2018) 054, [1708.04188](#).
- [39] CMS, “Search for heavy resonances decaying into two Higgs bosons or into a Higgs boson and a W or Z boson in proton-proton collisions at 13 TeV”, *JHEP* **01** (2019) 051, [1808.01365](#).
- [40] CMS, “Search for production of Higgs boson pairs in the four b quark final state using large-area jets in proton-proton collisions at $\sqrt{s} = 13$ TeV”, *JHEP* **01** (2019) 040, [1808.01473](#).
- [41] CMS, “Search for resonances decaying to a pair of Higgs bosons in the $b\bar{b}q\bar{q}'\ell\nu$ final state in proton-proton collisions at $\sqrt{s} = 13$ TeV”, *JHEP* **10** (2019) 125, [1904.04193](#).
- [42] CMS, “Search for resonant pair production of Higgs bosons in the $bbZZ$ channel in proton-proton collisions at $\sqrt{s} = 13$ TeV”, *Phys. Rev. D* **102** (2020) 032003, [2006.06391](#).
- [43] CMS, “Search for a heavy Higgs boson decaying into two lighter Higgs bosons in the $\tau\tau b\bar{b}$ final state at 13 TeV”, *JHEP* **11** (2021) 057, [2106.10361](#).
- [44] ATLAS, “Search for Higgs boson pair production in the $b\bar{b}WW^*$ decay mode at $\sqrt{s} = 13$ TeV with the ATLAS detector”, *JHEP* **04** (2019) 092, [1811.04671](#).
- [45] ATLAS, “Reconstruction and identification of boosted di- τ systems in a search for Higgs boson pairs using 13 TeV proton-proton collision data in ATLAS”, *JHEP* **11** (2020) 163, [2007.14811](#).
- [46] ATLAS, “Search for Higgs boson pair production in the $\gamma\gamma WW^*$ channel using pp collision data recorded at $\sqrt{s} = 13$ TeV with the ATLAS detector”, *Eur. Phys. J. C* **78** (2018) 1007, [1807.08567](#).
- [47] ATLAS, “Search for Higgs boson pair production in the $\gamma\gamma b\bar{b}$ final state with 13 TeV pp collision data collected by the ATLAS experiment”, *JHEP* **11** (2018) 040, [1807.04873](#).
- [48] ATLAS, “Search for resonant and non-resonant Higgs boson pair production in the $b\bar{b}\tau^+\tau^-$ decay channel in pp collisions at $\sqrt{s} = 13$ TeV with the ATLAS detector”, *Phys. Rev. Lett.* **121** (2018) 191801, [1808.00336](#).
- [49] CMS, “Combination of searches for Higgs boson pair production in proton-proton collisions at $\sqrt{s} = 13$ TeV”, *Phys. Rev. Lett.* **122** (2019) 121803, [1811.09689](#).

- [50] ATLAS, “Search for Higgs boson pair production in the $WW^{(*)}WW^{(*)}$ decay channel using ATLAS data recorded at $\sqrt{s} = 13$ TeV”, *JHEP* **05** (2019) 124, [1811.11028](#).
- [51] ATLAS, “Combination of searches for Higgs boson pairs in pp collisions at $\sqrt{s} = 13$ TeV with the ATLAS detector”, *Phys. Lett. B* **800** (2020) 135103, [1906.02025](#).
- [52] CMS, “Search for nonresonant Higgs boson pair production in final states with two bottom quarks and two photons in proton-proton collisions at $\sqrt{s} = 13$ TeV”, *JHEP* **03** (2021) 257, [2011.12373](#).
- [53] H. Abouabid et al., “Benchmarking Di-Higgs Production in Various Extended Higgs Sector Models”, (2021), [2112.12515](#).
- [54] CMS, “Search for a doubly-charged Higgs boson with $\sqrt{s} = 8$ TeV pp collisions at the CMS experiment”, (2016), CMS-PAS-HIG-14-039.
- [55] ATLAS, “Search for new phenomena in events with three or more charged leptons in pp collisions at $\sqrt{s} = 8$ TeV with the ATLAS detector”, *JHEP* **08** (2015) 138, [1411.2921](#).
- [56] ATLAS, “Search for anomalous production of prompt same-sign lepton pairs and pair-produced doubly charged Higgs bosons with $\sqrt{s} = 8$ TeV pp collisions using the ATLAS detector”, *JHEP* **03** (2015) 041, [1412.0237](#).
- [57] CMS, “A search for doubly-charged Higgs boson production in three and four lepton final states at $\sqrt{s} = 13$ TeV”, (2017), CMS-PAS-HIG-16-036.
- [58] ATLAS, “Search for doubly charged Higgs boson production in multi-lepton final states with the ATLAS detector using proton–proton collisions at $\sqrt{s} = 13$ TeV”, *Eur. Phys. J. C* **78** (2018) 199, [1710.09748](#).
- [59] ATLAS, “Search for doubly and singly charged Higgs bosons decaying into vector bosons in multi-lepton final states with the ATLAS detector using proton-proton collisions at $\sqrt{s} = 13$ TeV”, *JHEP* **06** (2021) 146, [2101.11961](#).
- [60] CMS, “Analysis of the CP structure of the Yukawa coupling between the Higgs boson and τ leptons in proton-proton collisions at $\sqrt{s} = 13$ TeV”, (2021), [2110.04836](#).
- [61] H. Bahl et al., “Constraining the \mathcal{CP} structure of Higgs-fermion couplings with a global LHC fit, the electron EDM and baryogenesis”, *Eur. Phys. J. C* **82** (2022) 604, [2202.11753](#).
- [62] CMS, “Combined measurements of Higgs boson couplings in proton–proton collisions at $\sqrt{s} = 13$ TeV”, *Eur. Phys. J. C* **79** (2019) 421, [1809.10733](#).
- [63] ATLAS, “Combined measurements of Higgs boson production and decay using up to 80 fb^{-1} of proton-proton collision data at $\sqrt{s} = 13$ TeV collected with the ATLAS experiment”, *Phys. Rev. D* **101** (2020) 012002, [1909.02845](#).
- [64] CMS, “Evidence for off-shell Higgs boson production and first measurement of its width”, (2021), CMS-PAS-HIG-21-013.
- [65] T. D. Lee, “A Theory of Spontaneous T Violation”, *Phys. Rev. D* **8** (1973) 1226, ed. by G. Feinberg.
- [66] J. E. Kim, “Weak Interaction Singlet and Strong CP Invariance”, *Phys. Rev. Lett.* **43** (1979) 103, UPR-0120T.

- [67] G. C. Branco et al., “Theory and phenomenology of two-Higgs-doublet models”, [Phys. Rept. **516** \(2012\) 1, 1106.0034](#).
- [68] F. Arco, S. Heinemeyer, and M. J. Herrero, “Triple Higgs couplings in the 2HDM: the complete picture”, [Eur. Phys. J. C **82** \(2022\) 536, 2203.12684](#).
- [69] ATLAS, “Combined measurements of Higgs boson production and decay using up to 139 fb⁻¹ of proton-proton collision data at $\sqrt{s} = 13$ TeV collected with the ATLAS experiment”, (2021), ATLAS-CONF-2021-053.
- [70] CMS, “Measurement of Higgs boson production and decay to the $\tau\tau$ final state”, (2019), CMS-PAS-HIG-18-032.
- [71] ATLAS, “Measurement of Higgs boson decay into b -quarks in associated production with a top-quark pair in pp collisions at $\sqrt{s} = 13$ TeV with the ATLAS detector”, [JHEP **06** \(2022\) 097, 2111.06712](#).
- [72] T. Biekötter and M. Pierre, “Higgs-boson visible and invisible constraints on hidden sectors”, (2022), [2208.05505](#).
- [73] R. Harlander et al., “Interim recommendations for the evaluation of Higgs production cross sections and branching ratios at the LHC in the Two-Higgs-Doublet Model”, (2013), [1312.5571](#).
- [74] M. Mühlleitner et al., “ScannerS: Parameter Scans in Extended Scalar Sectors”, (2020), [2007.02985](#).
- [75] ATLAS, “Search for heavy diboson resonances in semileptonic final states in pp collisions at $\sqrt{s} = 13$ TeV with the ATLAS detector”, [Eur. Phys. J. C **80** \(2020\) 1165, 2004.14636](#).
- [76] ATLAS, “Search for pair production of Higgs bosons in the $b\bar{b}b\bar{b}$ final state using proton-proton collisions at $\sqrt{s} = 13$ TeV with the ATLAS detector”, [JHEP **01** \(2019\) 030, 1804.06174](#).
- [77] ATLAS, “Combination of searches for heavy resonances decaying into bosonic and leptonic final states using 36 fb⁻¹ of proton-proton collision data at $\sqrt{s} = 13$ TeV with the ATLAS detector”, [Phys. Rev. D **98** \(2018\) 052008, 1808.02380](#).
- [78] ATLAS, “Search for heavy Higgs bosons decaying into two tau leptons with the ATLAS detector using pp collisions at $\sqrt{s} = 13$ TeV”, [Phys. Rev. Lett. **125** \(2020\) 051801, 2002.12223](#).
- [79] P. Bechtle et al., “Probing the Standard Model with Higgs signal rates from the Tevatron, the LHC and a future ILC”, [JHEP **11** \(2014\) 039, 1403.1582](#).